Proceedings of the 28th IEEE
EMBS Annual International Conference
New York City, USA, Aug 30-Sept 3, 2006

Comparison of Wave-Equation Versus Measurement-Processing Transducer Calibration for Ultrasonic Transmission Tomography

Jiri Zacal, Dusan Hemzal, Jiri Jan, Adam Filipik, Radovan Jirik and Radim Kolar

Abstract— **The contribution deals with the first step in using proper wave-equation based ultrasound propagation model in image reconstruction from the ultrasonic computed tomography data. Particularly, it compares the transducer calibration results obtained via direct measurement of the empty image field and consequential data processing based on a simple direct-propagation model with the simulation results obtained via solving the single-frequency wave equation under proper border conditions reflecting the realistic measurement geometry. The results show a reasonable qualitative agreement when a certain degree of phase-shifted coupling from the transmitting transducer elements to the neighbouring elements of the transducer field is admitted.**

I. Introduction

The transmission ultrasonic computed tomography (USCT) is an imaging modality based on simultaneous measurement of responses of many transducers surrounding the imaged object in a circular manner (in 2D case – Fig.1, or cylindrical in 3D) while one of the transducers is emitting an ultrasonic impulse. Gradually, each transducer becomes transmitting, and this way, a large set of signal data is obtained carrying the desirable information on the parametric field inside the circle to be imaged. Such a system, as experimentally developed in Forschungszentrum Karlsruhe [1], is primarily aimed at breast imaging.

In the first approximation, all the transducers are equally effective and their directional responses are omnidirectional – circular (or spherical, in 3D). Based on this hypothesis, interesting results have been obtained in image reconstruction area [2]. However, these assumptions are obviously not exact, and including more realistic transducer parameters in the image reconstruction promises a substantial improvement in the image quality. In [9], a method to calibrate the individual transducers in terms of their directional characteristics (frequency and direction dependent radiation function) and individual transducer efficiencies has been suggested (for more details, see below), based on a simple model of ultrasound transmission and deriving the parameters computationally via solving an extensive system of linear equations. The results provided there seem reasonable, and also a comparison with a hydrophone measurement of a directional characteristic has shown a good qualitative agreement.

However, there is a discrepancy between the computed characteristics and the basic radiation theory: the calculated characteristics contain substantial side-lobes while theoretically only a single main lobe should be present taking into account the small concrete geometrical dimensions of the transducers. In order to try resolve this problem, we applied a completely independent approach to directional characteristics computation, which enables in principle to take into account not only possibly uneven distribution of both amplitude and phase on the transducer surface but namely also a coupling between neighbouring transducers leading to attenuated and phase shifted contributions to the radiated field. Besides leading to satisfactory (though still preliminary) conclusion that such a coupling may be the explanation for the discrepancy, thus confirming at least qualitatively the correctness of the measurement-processing approach [9], the wave-equation based simulation is the first step on the prospective way to an alternative approach to image reconstruction utilising an iterative solution of the inverse problem encompassing repeated wave equation solution.

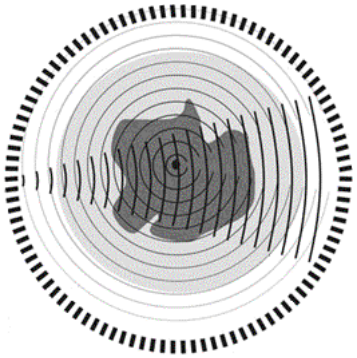

Fig. 1. Circular arrangement of transducers in a USCT system [1]: in each measurement step, one transducer is transmitting while others are receiving the transmitted and scattered signals

II. Methods

A. The measurement-processing calibration

The calibration method, as in a greater detail described in [9], utilises a series of wide-band (impulse) measurements with the image field empty (only plain water). The signals received by individual transducers are modelled in spectral domain (via DFT decomposition) by the amplitude spectrum of the signal received by the receiver *r* and using emitter *e* as

Manuscript received April 2, 2006. This project is running under the support of the national research centre DAR (sponsored by the Ministry of Education, Czech Republic), project no. 1M6798555601.

J.Zacal, J.Jan, A.Filipik, R.Jirik and R.Kolar are with the Dept. of Biomedical Eng., FEEC, Brno University of Technol., (corresp. author J. Zacal, zacal@feec.vutbr.cz), D.Hemzal is with the Inst. for Theoretical Physics & Asptrophysics, Masaryk University, Brno, Czech Republic.

$$S_{e,r}(f) \cong R_e(f, \vartheta_{e\to r}) \cdot R_r(f, \vartheta_{e\leftarrow r}), \qquad (1)$$

where $R_e(f, \vartheta_{e\to r})$, $R_r(f, \vartheta_{e\leftarrow r})$ are the radiation functions of the emitter and of receiver, respectively, f is the frequency, $\vartheta_{e\to r}$ is the angle with respect to receiver axis, and $\vartheta_{e\leftarrow r}$ is the angle with respect to emitter. The computation of the radiation Taking each emitter – receiver – frequency combination, a system of equations can be constructed and log-linearized:

$$\log\left(S_{e,r}(f)\right) = \log\left(R_e(f, \vartheta_{e\to r})\right) + \log\left(R_r(f, \vartheta_{e\leftarrow r})\right). \quad (2)$$

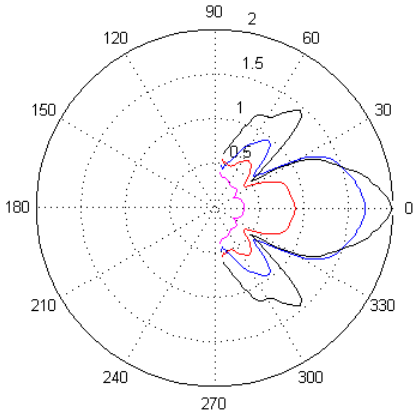

Fig. 2. MP-calculated directivity characteristics for individual frequencies (f = 3 MHz for the maximal curve)

The radiation functions are further decomposed into

$$R(f, \vartheta) = s \cdot D(f, \vartheta), \qquad (3)$$

where s is an individual multiplicative constant (efficiency in emitting mode or sensitivity in receiving mode) both supposedly equal (or proportional), representing a fatigue and material flaws of individual transducers, while the directivity function $D(f, \vartheta)$ can be assumed common to all elements thanks to their equal geometry. Solution of the system (2) taking into account (3) provides the unknown parameters of the sensors. For N transducers with N-1 possible emitting/receiving angles and M frequency bands, N x (N-1) x M equations can be stated with the same number of unknown parameters. However, given the limitations of the experimental setup, further assumptions had to be introduced in order to obtain a determined equation system, most important among them the identical shape and axial symmetry of $D(f, \vartheta)$ for all transducers. Solving the obtained system, the results were obtained in the form of a map of directivity function $D(f, \vartheta)$ (see Fig. 2 and 3), and also of individual efficiencies, not important in the context of this paper.

B. *Wave equation approach*

Theoretical background: The space- and time-dependent local condition of the intermediate medium, which is degassed water here, can be characterised by thermo-dynamical state quantities (mass density ρ, pressure p, absolute temperature T), along with the dynamical model, for which the non-viscous fluid is taken here, bringing in terms of strain tensor $\boldsymbol{\tau}$, $\tau_{ij} = -p\delta_{ij}$. Throughout the article, only entropy conserving processes are considered, of which the usually considered adiabatic process is a special case. As a consequence, the state equation is expressible in the form $p = p(\rho)$, which in the vicinity of equilibrium values p_0, ρ_0 gives

$$p \approx p_0 + \left(\frac{\partial p}{\partial \rho}\right)_0 (\rho - \rho_0) \equiv p_0 + c^2(\rho - \rho_0). \qquad (4)$$

As the medium is treated as compressible, it shows the wave phenomena in the following way. Denoting by p', ρ' the state quantities equilibrium deviations $p = p_0 + p'$, $\rho = \rho_0 + \rho'$, the equations of motion reduce for small deviations to the wave equation (WE)

$$\frac{\partial^2 p'}{\partial t^2} - c^2 \Delta p' = 0. \qquad (5)$$

The same equation rules the density deviation ρ' behaviour, as well as temperature deviation T' and behaviour of the media element displacement speed field $\mathbf{v}$.

The transducer action is realised as harmonic oscillation $\mathbf{u_0}$ of the media element displacement field $\mathbf{u}$, $\mathbf{v} = \partial\mathbf{u}/\partial t$, perpendicular to appropriate region of equipment border. The relation between border condition for displacement speed $\mathbf{v_0}$ and, say, pressure deviation border behaviour p'_0 is however non-local, i.e. the pressure border condition cannot be stated from border behaviour of displacement speed only et vice versa – the whole solution to wave equation is always involved. Yet, as an approximation, the harmonic oscillation of pressure deviation on the transducer is assumed. Considering only dynamically stationary (single frequency ω) solutions, $p' = \overline{p}' \exp(\mathrm{i}\omega t)$ and thus the Helmholtz equation is obtained,

$$\omega^2 \overline{p}' + c^2 \Delta \overline{p}' = 0, \qquad (6)$$

and similarly for dynamically stationary parts of other quantities. As for border conditions on a single transducer chosen, $\overline{p}'_0$ is a constant then, providing even distribution of the amplitude and phase on its surface. For the numerical finite-element solution, the field area must be surrounded by a curve carrying the non-reflecting border condition.

As an output there stand the values of a module $\overline{p}\,\overline{p}^*$ of pressure deviation field over a circle with sufficiently large radius centred in the emitting transducer(s); * stands for complex conjugation. These values, if normalised to the highest value, may serve as approximation of the sought far field radiation pattern of the configuration geometry chosen.

Wave-equation based simulations: The model corresponding to (5) including both kind of the border conditions has been implemented in the MATLAB® 7.1 (R14) environment running on a Intel Pentium 4, 3GHz (HT), 4GB RAM under Windows XP®. The core of the finite element solution has been using the MATLAB's Partial Differential Equation (PDE) Toolbox 1.0.4. The oscillations according to (5) are generally modelled by the WE formulation

$$\mathtt{U(x,y,t)''= div(grad(U))}, \quad (7)$$

in which the time-dependence is eliminated as the wave is monochromatic, so that the solution is expected in the factored form

$$\mathtt{U(x,y,t) = exp(2*i*k*t*pi)*u(x,y)}. \quad (8)$$

This way reduced problem acquires the form of eliptic equation, particularly *Helmholtz equation* expressed in the framework of the PDE Toolbox as

$$\mathtt{-4*pi^2*k^2*u = div(grad(u))}. \quad (9)$$

Three types of boundary conditions are involved in the present formulation: solid walls, entries and exits. On the reflective walls there are no oscillations, thus the boundary condition is just **`u=0`**. At the outer perimeter of the solution area, the absorbing boundary condition must be formulated, which provides for zero reflections (simulated infinite surroundings). This turns out to be equivalent to the Neumann condition

$$\mathtt{n*grad(u)=-2*pi*i*k*u}, \quad (10)$$

where **`n`** is the outward-pointing normal. At the entrance (excitation transducer surface), Dirichlet boundary condition **`u=const.`** is applied.

The used the wavelength was 0.5 mm (f=3 MHz), therefore the wave number **`k=2`**. The solution has been achieved by calling the function (see [8] for *b,p,e,t* definition)

$$\mathtt{u=assempde(b,p,e,t,1,(2*pi*i*k)^2,0).} \quad (11)$$

In order to evaluate the radiation function via finite element model, a 2D finemesh (~235.000 nodes, ~465.000 elements) has been created, with 16 nodes per wavelength at minimum.

III. Results and Discussion

The WE solution has provided a series of results needed for comparison with the measurement-processing (MP) approach. The isolated single-transducer solution gives the theoretically expected one-lobe directionality, as seen on Figs. 3 and 4; the lobe half-amplitude width is nevertheless similar to that of the MP result. In order to verify the hypothesis that the MP determined and measured side lobes are the consequence of mechanical or even electrical coupling, series of WE solutions has been provided, with different amplitudes and phase shifts of oscillations on the nearest neighbours' surfaces (particularly detailed in the range of $\pm 0.7 \pm i0.7$ of the central transducer constant amplitude). Particularly, in the vicinity of $-0.45+ i\,0.75$ to $-0.75 + i\,0.75$ (Figs. 5–7), the directional characteristics show the behaviour qualitatively similar to the MP result, with the best match in Fig. 6, the complete WE solution of

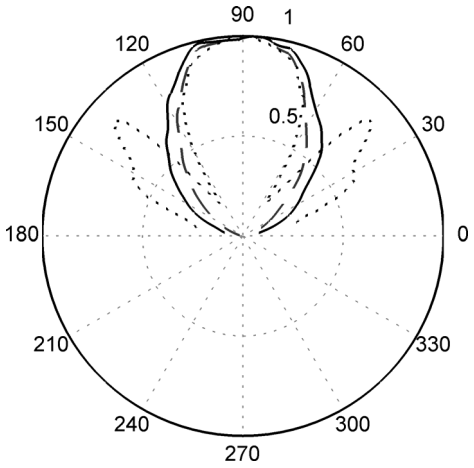

Fig. 3 Directional characteristics of a single transducer (dashed curve – WE simulation, solid curve – WE distance corrected, dotted curve – MP calculated)

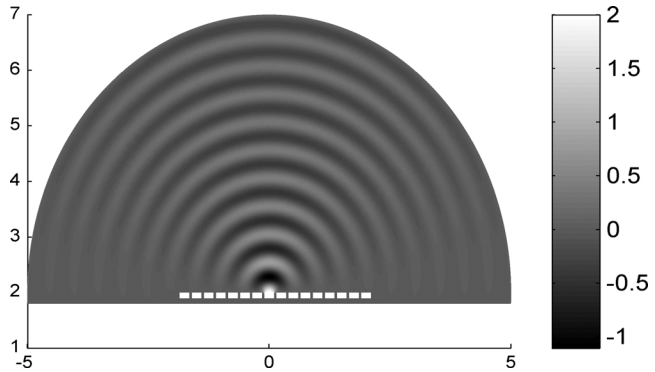

Fig.4. WE field complete solution corresponding to Fig. 3.

which is on Fig. 8. As for the difference in the sharpness of minima, this can be explained by probable existence of more complicated excitation pattern with an uneven phase distribution in contrast to the three-area approximation as used in the WE solution.

The WE results, particularly considering the Fig. 7, seem to confirm the hypothesis that the strange (with respect to theoretical expectations) shape of the MP determined directional characteristics (splitting of the main lobe into three lobes with relatively strong side lobes) may be caused by some coupling from the excited transducer to the neighbouring ones, due to either mechanical binding or(/and) a cross-over on the electrical side. Though still preliminary, this is a satisfactory conclusion, in principle admitting the correctness of the MP approach that was challenged by the above mentioned discrepancy.

Moreover, this work was intended as the first attempt to an alternative approach to the USCT data analysis. The positive experience with the WE - FEM approach based on the strict physical formulation, although so far limited to the Helmholtz case, is promising with respect to the prospective use of more complex formulation taking into account also the spatially variable attenuation phenomena in the

ultrasound field. This should enable a basically different approach to the image reconstruction from the USCT data, based on the iterative inverse problem solution modelling in each step the complete time- and space-dependent ultrasonic field.

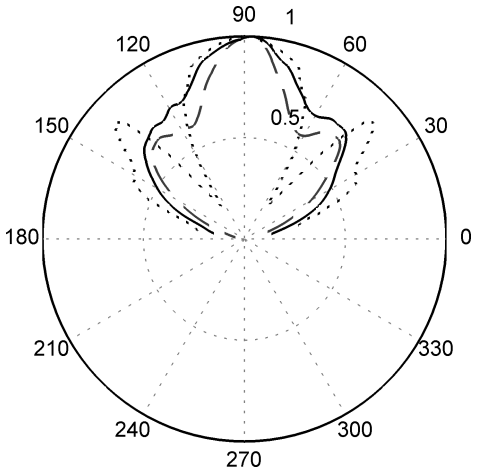

Fig. 5. Directional characteristics for the case of three-element radiation (coupling to the nearest neighbours causing the oscillation with -0.45+*i*0.75 of the central transducer excitation).

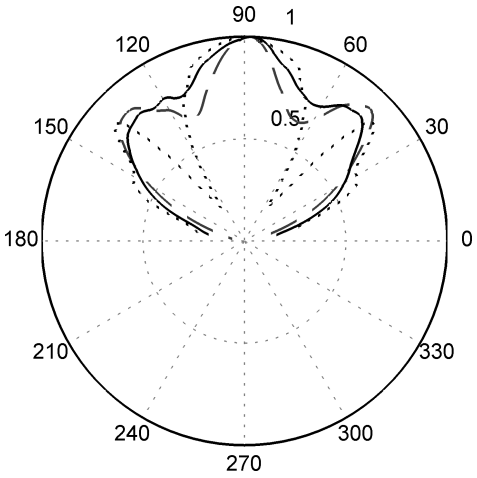

Fig. 6. Similarly as in Fig. 5, for -0.6+*i*0.75

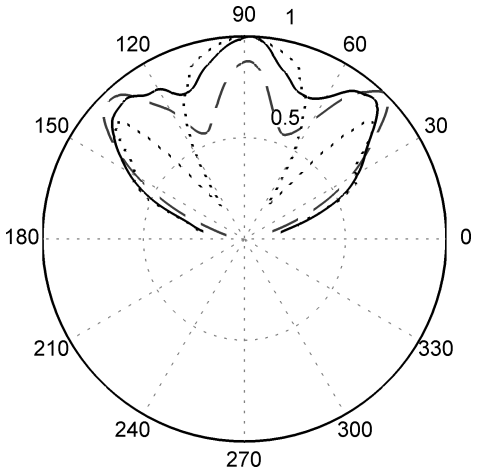

Fig.7. Similarly as in Fig. 5, for -0.75+*i*0.75

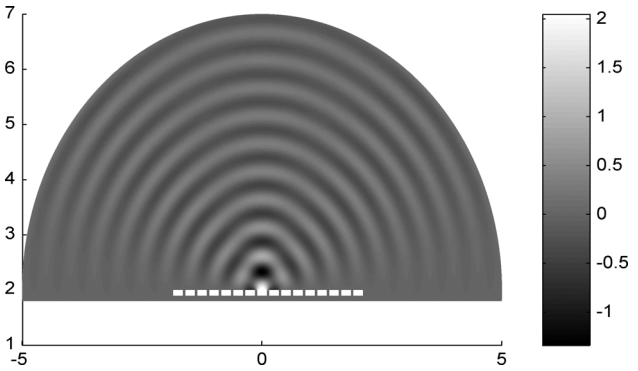

Fig.8. WE field solution corresponding to Fig. 6. Below, the row of 16 transducers is situated, of which the three near centre are active

IV. Conclusions

The short contribution describes the alternative method of USCT data analysis based on proper wave equation formulation. It turns out that this way provided results concerning the directivity properties of transducers used in transmission ultrasonic tomography confirmed – at least qualitatively – the correctness of the previous calibration procedure utilising a simpler model of ultrasound propagation. The results based on this simplified measurement-processing approach, provided by solving the corresponding extensive linear equation model that seemed to violate the basic radiation theory, can be explained using the results of the more general wave-equation solution. The wave-equation based approach may thus be considered a promising alternative tool for USCT data analysis, with potentially a higher degree of realism.

Acknowledgement

Authors sincerely acknowledge the contribution of Dr Rainer Stotzka and Dr Nicole Ruiter, both of Forschungszentrum Karlsruhe Germany, who are the authors of the experimental USCT system and provided the data used in the paper.

References

[1] STOTZKA,R., RUITER,N. et al. (2002): Medical Imaging by Ultrasound-Computertomography. Proc. of SPIE Medical Imaging. 2002., pp. 25

[2] JIRIK R., STOTZKA R, TAXT T. (2005): Ultrasonic Attenuation Tomography Based on Log-Spectrum Analysis. Proceedings of SPIE, Medical Imaging 2005 conf. Volume: 5750, pp. 305-314.

[3] MULLER, T.O. et al.: Ultrasound computertomography: image reconstruction using local absorption and sound speed profiles. Proc. of ESEM - European Society for Engineering and Medicine, 2003.

[4] MING L.: USCT image reconstruction regarding object and sensor properties. MSc thesis, Univ. of Applied Science Karlsruhe, 2003.

[5] B.A.J.Angelsen: Ultrasound Imaging – Waves, Signals and Signal Processing. Emantec 2000

[6] PRESS, W. H. et al. (2002): Numerical Recipes in C, The Art of Scientific Computing (2nd ed.), Cambridge University Press, 2002.

[7] MATLAB® v. 7.1 (R14) manual, Mathworks 2005 (www.mathworks.com/ products/matlab)

[8] MATLAB® PDE - Toolbox v. 1.0.4 manual, Mathworks 2005 (www.mathworks.com/products/pde)

[9] FILIPIK, A., JAN, J., JIRIK, R. Transducer Calibration in Transmission Ultrasound Tomography In Proc. of 3rd EMBEC'05, Prague: CD version, paper no. 2650. IFMBE, 2005